https://doi.org/10.31925/farmacia.2024.5.10 **ORIGINAL ARTICLE**

A QUALITY-BY-DESIGN APPROACH FOR OPTIMISATION OF ACTIVE INGREDIENT TRANSFEROSOMAL FORMULATIONS

FLORENTINA-IULIANA COCOȘ [1,2], RĂZVAN-MIHAI PRISADA [1,2]*, VALENTINA ANUȚA [1,2], LĂCRĂMIOARA POPA [1,2], MIHAELA-VIOLETA GHICA [1,2], RADU-CLAUDIU FIERĂSCU [3,4], BOGDAN TRICĂ [3], CRISTIAN-ANDI NICOLAE [4], CRISTINA-ELENA DINU-PÎRVU [1,2]

[1]*Department of Physical and Colloidal Chemistry, Faculty of Pharmacy, "Carol Davila" University of Medicine and Pharmacy, 020956, Bucharest, Romania*

[2]*Innovative Therapeutic Structures Research and Development Centre (InnoTher), "Carol Davila" University of Medicine and Pharmacy, 6 Traian Vuia Street, 020956, Bucharest, Romania*

[3]*National Institute for Research & Development in Chemistry and Petrochemistry – ICECHIM Bucharest, 202 Spl. Independenței, 060021, Bucharest, Romania*

[4]*Faculty of Chemical Engineering and Biotechnology, "Politehnica" National University of Science and Technology Bucharest, 1-7 Gh. Polizu Street, 011061, Bucharest, Romania*

**corresponding author: razvan.prisada@umfcd.ro*

Manuscript received: June 2024

Abstract

This research investigated the design, characterization and optimization of active ingredient-loaded transfersomes for enhanced transdermal delivery in the treatment of skin cancer. A systematic formulation development approach, guided by the principles of Design of Experiments (DoE) and One Factor At a Time (OFAT), was employed to optimize the formulation parameters. Physicochemical properties including particle size, polydispersity index (PDI), zeta potential and entrapment efficiency were comprehensively assessed to ensure the stability and drug-loading capacity of the transfersomes. Morphological analysis using Scanning Electron Microscopy (SEM) and Transmission Electron Microscopy (TEM) confirmed well-defined transfersome structures. *In vitro* release kinetics studies demonstrated a controlled and sustained release profile of active ingredient from the transfersomes, highlighting its potential for enhanced therapeutic efficacy.

Rezumat

Această cercetare are la bază proiectarea, caracterizarea și optimizarea transferozomilor cu active ingredient pentru o eliberare transdermică îmbunătățită în tratamentul cancerului de piele. O abordare sistematică de dezvoltare a formulării, ghidată de principiile Designului de Experimente (DoE) și a modificării unui singur parametru o dată (OFAT), a fost utilizată pentru optimizarea parametrilor formulării. Proprietățile fizico-chimice, inclusiv dimensiunea particulelor, indicele de polidispersie (PDI), potențialul zeta și eficiența de încapsulare, au fost evaluate exhaustiv pentru a asigura stabilitatea și capacitatea de încărcare a medicamentului a transferozomilor. Analiza morfologică folosind microscopia electronică de scanare (SEM) și microscopia electronică de transmisie (TEM) a confirmat structuri bine definite ale transferozomilor. Studiile de cinetică a eliberării *in vitro* au demonstrat un profil de eliberare controlat și susținut al docetaxelului din transferozomi, evidențiind potențialul său pentru o îmbunătățirea eficacității terapeutice.

Keywords: active ingredient, anticancer agent, transfersomes, nanoencapsulation, transdermal drug delivery, design of experiments

Introduction

Active ingredient (DTX) is a semi-synthetic taxane second-generation anti-neoplastic agent derived from *Taxus baccata* [1-3]. The mechanism of taxane derivates is represented by irreversible binding to β-actin, having as a consequence the alteration of the micro-tubule polymerization and disruption of cell mitosis, resulting in apoptosis and, finally, cytotoxicity [2-4]. The Food and Drug Administration (FDA) and the European Medicines Agency (EMA) have approved more medicinal products containing active ingredient as active pharmaceutical ingredients, such as active ingredient and active ingredient®. Among their indications can be listed different types of cancer, such as breast cancer, ovarian cancer, prostate cancer, non-small cell lung cancer, gastric adenocarcinoma, head and neck cancer, including hormone-refractory metastatic types [5-7]. Over the years, several adverse reactions were reported for this active pharmaceutical ingredient, such as severe allergic reactions and system toxicity [1, 2, 8, 9], such as hypotension, bronchospasm, urticaria [9], morbidity related to the intravenous access site, risk of catheter-related infections, thrombosis, extravasation [2] and fluid retention [1].

DTX presents a low solubility in water (4.93 μg/mL) [1, 3, 4, 8] and high lipophilicity with a value for logP of 4.1 [1, 8]. To combat these pharmaceutical inconvenient, surfactants, such as Tween 80, or alcohol

can be added into formulations [1, 2, 9], a fact noted in available commercial formulations, Active ingredient and Duopafei®. Polysorbate 80 and ethanol have been associated with a series of adverse reactions, including severe hypersensitivity, neutropenia, nonallergic anaphylaxis, rash, injection and infusion-site adverse events (pain, erythema, thrombophlebitis), fluid retention and alopecia [10-13]. Moreover, it has been demonstrated that these two excipients lead to the accumulation of DTX in healthy tissues and organs , thus causing systemic toxicity. The severity of all these adverse effects caused both by the active substance and excipients may lead to interruption of the treatment [10, 14, 15].

Therefore, overcoming the formulation and clinical disadvantages of DTX and increasing the bio-availability of the active pharmaceutical ingredient to the tumour has been a focus of development studies of nanocarriers. Thus, among the tested nanoformulations can be mentioned liposomes [16-19], lipid nanoparticles [3, 8, 20-23] and nanomicelles [11].

Another way to overcome all these drawbacks of DTX in clinical use is through nanoformulations, such as liposomes, nanoemulsions, nanoparticles, and so on.

Ultradeformable vesicular system or transfersomes, introduced by Gregor Cevc in the 1990s [24-27], are self-optimising nanodrug carrier systems capable of dermal and transdermal delivery of hydrophilic, hydrophobic and amphiphilic active ingredient substances [25, 28]. The modified liposomal vesicular system composition includes a phospholipidic component natural (such as egg phosphatidylcholine, soybean phosphatidylcholine) or synthetic (such as dipalmitoyl phosphatidyl glycerol, dipalmitoyl phosphatidylcholine, dimyristoyl phosphatidylcholine), a bilayer softening component called edge activator (such as Tweens, Spans, sodium cholate, sodium deoxycholate, oleic acid, dipotassium glycyrrhizinate) and hydrating medium represented by water, alcoholic solution containing about 3 - 10% of ethanol or saline phosphate buffer at different values of pH [24-26, 28-32].

The transferosomal unique structure makes them capable of delivering various therapeutic agents with a wide range of solubility, such as peptides [29, 33, 34], active ingredient [34, 35], corticosteroids [36-38], anaesthetics [39, 40], NSAIDs [41-43], anticancer drugs [24, 27] and herbal drugs [28]. Due to their ultra-deformability and elastic properties, these drug carriers can squeeze themselves through constrictions of the skin barrier, so active compounds are transported across the skin without any measurable loss [25, 29, 44].

Transfersomes are ultra-deformable vesicles capable of penetrating the skin's stratum corneum, thus enabling enhanced local drug delivery. This unique characteristic allows for the direct administration of DTX to the tumour site, potentially increasing drug concentration at the target site while minimising systemic exposure.

The objective of this study was to develop transfersomes with DTX and to optimise their characteristics to obtain a suitable system for trans-dermal delivery by applying the Quality by Design (QbD) principles. The development and optimisation processes are carried out through experimental designs (Design of Experiments - DoE). The current study explores the formulation and evaluation of DTX-loaded transfersomes for local administration in the treatment of skin cancer. This innovative approach aims to improve therapeutic efficacy, reduce side effects and offer a significant advancement in skin cancer treatment. By leveraging the enhanced permeation capabilities of transfersomes, this research highlights a novel and promising strategy for localised chemo-therapy, potentially setting a new benchmark in the field of topical cancer treatments.

Materials and Methods

Materials

For transfersomes preparation the following substances were used: active ingredient (ScinoPharm, Taiwan), phospho-lipon 90G (Lipoid GmbH, USA), Span 80, chloroform for analysis, oleic acid (Merck, USA), cholesterol, sodium deoxycholate, sodium cholate (Sigma-Aldrich, USA), Tween 80, active ingredien monobasic, methanol for HPLC gradient grade (Honeywell, USA), disodium phosphate (Chemical, Romania). The other reagents used for analysing the obtained formulations 5 rade -Honeywell, formic acid-Honeywell, sodium chloride - Chimactiv,potassium chloride - Lach:ner, water for chromatographic use) had analytical purity.

5-Fluorouracyl (5-FU), PBS/1 mM EDTA, L-glutamine (Glu), active ingredient (100 units/mL), active ingredient (100 μg/mL), Dulbecco's modified Eagle's medium (DMEM), foetal bovine serum (FBS), propidium iodide (PI) (stock solution 4 mg /mL PI in PBS) and RNase A (stock solution 10 mg/mL RNase A) were purchased from Sigma Aldrich (St. Louis, MO, USA).Annexin V-FITC kit and CycleTEST PLUS DNA Reagent kit were purchased from Becton Dickinson Biosciences (San Jose, CA 95131, USA).

Preparation of transfersomes

DTX-loaded transfersomes (Tr-DTX) were prepared using a lipid-based film hydration method [25, 27, 39, 40] (Figure 1). Briefly, lipids, surfactants and DTX were solubilised in chloroform/methanol (2:1, v/v) in a round bottom flask and mixed well. The organic solvent was evaporated under reduced pressure in a rotary evaporator until a thin film was formed. After completing residual solvent evaporation under reduced pressure, the film was hydrated with phosphate buffer pH 7.4 using a rotary evaporator. Then, the suspension was sonicated using a probe sonicator (Hielscher, UP200Ht, Germany) to obtain small vesicles. Subsequently, the sonicated transfersomes

were homogenized by extrusion through a 100 nm polycarbonate membrane using a jacketed extruder (Jacketed liposome extruder, Genizer, United States). After that, the obtained formulation was purified by dialysis in phosphate buffer pH 7.4 at room temperature overnight. In a similar mode, for the optimum formulation, Tr-Blank, without DTX, was prepared.

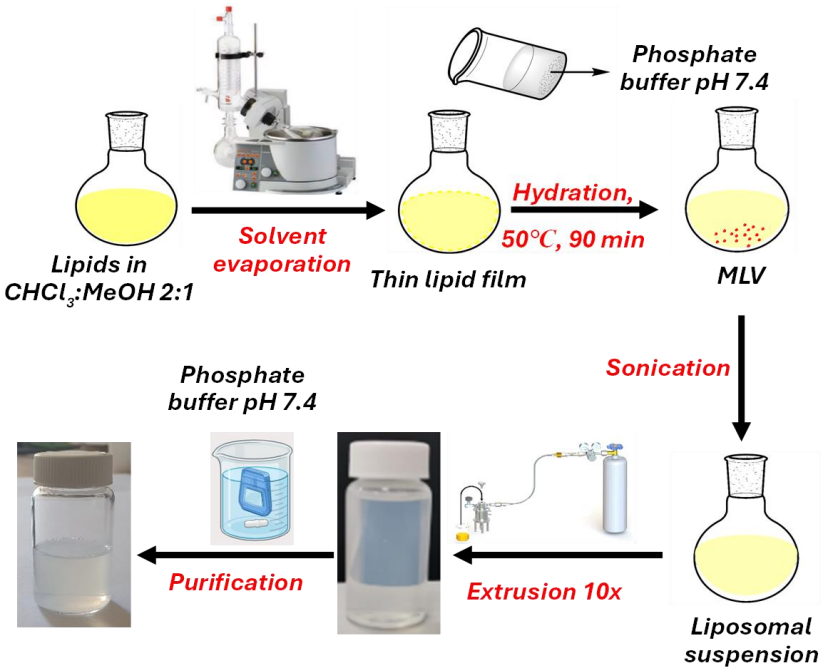

Figure 1.
Schematic representation of film hydration method

Table I
Experimental variables, levels and responses analysed in the Definitive Screening design

Continuous variables	Low level	High level
DTX (mg)	5	20
EA (mg)	5	30
RV (mL)	10	20
RTime (min)	60	120
RTemp (°C)	45	65
ST (min)	5	15
Categorical variables	**Levels**	
T80/DXC	T80 | 50:50 (w/w)	DXC
Ch	Yes	No
Responses	**Optimisation**	
Size (nm)	Minimum	
ZP (mV)	in range	
Release 8h (%)	Maximum	
Release 24h (%)	Maximum	
EE (%)	Maximum	
Recovery (%)	Maximum	

Experimental design

Utilising Design Expert software (version 13, USA), a Definitive Screening experimental design was implemented. Analysis of Variance (ANOVA) was utilised to determine the significance of the regression and identify the pivotal experimental factors (p-value < 0.05). Table I illustrates the independent variables, including the amount of DTX, the type of edge activator (only Tween 80 (T80), only sodium deoxycholate (DXC), or a mixture between T80 and DXC (50:50, w/w), the quantity of edge activator (EA), the rehydration volume (RV), the rehydration time (RTime), the rehydration temperature (RTemp), the sonication time (ST) and the presence of cholesterol in the formulation (Ch), along with their respective levels. Furthermore, the optimisation criteria used for the evaluated outcomes are detailed, encompassing transfersomal particle size before filtration (Size), zeta potential (ZP), the amount of DTX released after 8 hours (Release 8 h), respectively after 24 hours (Release 24 h), the entrapment efficiency (EE) and the quantity of DTX recovery after filtration (Recovery). The transfersomal particle size after filtration did not represent an evaluated response because all the formulations exhibited a value of approximately 100 nm. Table II provides comprehensive information regarding the 18 formulations.

To confirm the values obtained for recovery after filtration, DTX solutions were prepared and diluted in phosphate buffer pH 7.4, the rehydration medium of the transferosomes. These were maintained under continuous stirring for two hours, the maximum rehydration time tested in the DoE, at the tested rehydration temperatures (45°C, 55°C and 65°C). All the samples were then diluted properly and analysed using the HPLC method described below.

Table II

Definitive Screening design of Tr-DTX, showing the independent variables (DTX, RV, RTime, RTemp, ST, T80/DXC and Ch)

Formulation	A: DTX (mg)	B: T80/DXC	C: EA (mg)	D: RV (mL)	E: RTime (min)	F: RTemp (°C)	G: ST (min)	H: Ch
Tr_1	5.0	T80	17.5	10	60	65	5	No
Tr_2	20.0	T80	5.0	10	90	65	15	Yes
Tr_3	20.0	T80	30.0	10	120	45	5	No
Tr_4	12.5	T80	30.0	20	120	65	15	No
Tr_5	20.0	DXC	5.0	15	120	65	5	No
Tr_6	20.0	DXC	30.0	10	60	55	15	No
Tr_7	12.5	DXC	5.0	10	60	45	5	Yes
Tr_8	5.0	T80	5.0	20	120	55	5	Yes
Tr_9	12.5	50:50	17.5	15	90	55	10	No
Tr_10	20.0	50:50	30.0	20	60	65	5	Yes
Tr_11	5.0	DXC	30.0	10	120	65	10	Yes
Tr_12	20.0	DXC	17.5	20	120	45	15	Yes
Tr_13	5.0	50:50	5.0	10	120	45	15	No
Tr_14	20.0	T80	5.0	20	60	45	10	No
Tr_15	5.0	DXC	30.0	20	90	45	5	No
Tr_16	12.5	50:50	17.5	15	90	55	10	Yes
Tr_17	5.0	T80	30.0	15	60	45	15	Yes
Tr_18	5.0	DXC	5.0	20	60	65	15	Yes

The independent variables are also denoted by capital letters: A = DTX, B = T80/DXC, C = EA, D = RV, E = RTime, F = RTemp, G = ST and H = Ch.

One-Factor-at-a-Time-Experiments (OFAT)

Given the use of a broad screening design, additional tests are necessary to achieve an optimal stable formulation through one-factor-at-a-time (OFAT) adjustment. Factors such as the amount of DTX, including a new liquid lipid (oleic acid) and removing cholesterol were varied in these types of experiments. Each tested formulation and the response factors monitored are presented in Table III.

Table III

Results derived from OFAT experiments (Size, ZP, EE and Recovery)

Formulation	Variation	Size (nm)	ZP (mV)	EE (%)	Recovery (%)	Observation
F1	BOA	NT	NT	NT	NT	precipitation
F2	F1 with the difference: 15.0 mg DTX	NT	NT	NT	NT	precipitation
F3	F2 with the difference: 10.0 mg DTX	87.7	-1.59	46.92	70.93	-
F4	F3 with the difference: 12.5 mg DTX	84.7	-4.09	53.45	80.11	-
F5	F4 with the difference: 20 mg T80 and added 10 mg OA	111.4	-10.81	53.86	98.78	-
F6	F5 with the difference: 15.0 mg DTX	NT	NT	NT	NT	precipitation
F7	F5 with the difference: no cholesterol	117.2	-12.24	42.11	93.22	-
F8	F7 with the difference: 20.0 mg OA	90.7	-14.37	79.78	96.37	-

NT = not tested, OA = oleic acid

Transfersomes characterisation

Determination of DTX concentration. For the quantitative determination of DTX, a Jasco high-performance liquid chromatographer (HPLC) system was used, consisting of a quaternary pump model PU-4180, an autosampler AS-4150, a DAD detector model MD-4010 and a column thermostat model CO-4061. Separation was performed on a Kinetex C18 column, 2.6 µm, 100 x 3 mm, at 45°C, using a mobile phase composed of 0.1% formic acid (mobile phase A) and a mixture of acetonitrile:methanol 1:1 (mobile phase B). Elution was carried out using a gradient method, starting with a ratio of 45:55 (v/v, mobile phase A:mobile phase B) and continuing with a system wash with 95% mobile phase B to remove traces of fatty acids due to the composition of transferosomes from the column.

Dynamic light scattering (DLS). The investigation of transfersomal average hydrodynamic diameter and polydispersity index (PDI) employed the dynamic light scattering (DLS) technique on undiluted samples. Accurate measurements were carried out using a VascoKin particle analyser (Cordouan Technologies, France) equipped with a 638-nanometer laser.

Furthermore, the behaviour of particles was examined using an *in situ* head that operated in a back-scattering mode, employing a scattering angle of 170°. Calibration was performed using a standardised colloidal dispersion of 1% latex with particles measuring 100 nm. The size distribution (nm) based on intensity (a.u.)

was determined for each transfersomal formulation sample using the Cumulant algorithm, which is associated with the autocorrelation function expressed in time (μs) as a function of intensity (a.u.). The obtained results were fitted with the Rayleigh model [45, 46].

Zeta potential analysis. The analysis of zeta potential was performed using the laser doppler electrophoresis technique [47]. The measurements were conducted using the Wallis Zeta potential analyser (Cordouan Technologies, France), equipped with a 20 mW diode laser operating at a wavelength of 635 nm. A Ludox TM-50 colloidal silica 0.5% standard (Sigma Aldrich, USA) was used for the equipment calibration. The transfersomal formulation were diluted ten times for this analysis. The reported results correspond to the average values obtained from six determinations.

Entrapment efficiency. The encapsulated amount of active ingredient was determined through a direct method [48-52]. The samples were dialysed in phosphate buffer pH 7.4 overnight using Slide-A-Lyzer Dyalisis Cassette G2, 10,000 MWCO (Repligen, USA). Prior to the analysis, the cassette were prepared by immersing them for at least 30 minutes in a dialysis medium. Drug concentrations before and after purification were determined using the HPLC method described above.Encapsulation efficiency (EE %) was calculated using the following formula [53, 54]:

$$EE\ (\%) = \frac{Quantity\ of\ DTX\ in\ transfersomes}{Total\ amount\ of\ DTX} \times 100 \quad (1).$$

In vitro drug release study. An *in vitro* release of DTX study was performed using a dialysis method [26, 55-57]. USP apparatus 4 (Sotax CE7 smart with CY 7 piston pump, Sotax AG, Switzerland) with 12 mm diameter flow-through cells was used in a closed system for *in vitro* release testing. Therefore, 1.2 mL of transfersomal suspension were transferred into Float-A-Lyzer G2 Dialysis Devise, 50 kD MWCO (Repligen, USA), which were seated on glass beads with 1 mm diameter 250 mL of phosphate saline buffer pH 7.4 with 20% ethanol were circulated at a flow of 8 mL/min and maintained at a controlled temperature of 37°C [58]. At regular time intervals, one mL of sample was withdrawn and replaced with one mL of fresh medium. All the samples were analysed by HPLC method described above.

Scanning Electron Microscopy (SEM). In preparing SEM samples, a droplet of each transfersomal suspension was applied onto a conductive carbon tape (TED PELLA Inc., USA), securely affixed to an aluminium SEM stub. The subsequent step involved the sputter-coating of the samples with a gold-palladium target within an argon gas milieu to ensure sufficient electrical conductivity and compatibility with SEM examination. This sputter-coating process, conducted for a duration of 1 minute, employed a plasma current of 25 mA and utilised a SC7620 Mini Sputter Coater (Quorum Technologies, UK). Following the coating procedure, the samples were preserved in a desiccator until subjected to analysis. The evaluation of these samples was performed using a TM4000Plus scanning electron microscope (Hitachi, Japan), which operated at a voltage setting of 15 kV and utilised backscattered electron detection (BSE) mode for imaging.

Cryo-transmission electron microscopy (Cryo-TEM). The morphology of the transfersomes samples was verified using a Vitrobot Mark IV (Thermo Fisher Scientific, Waltham, MA, USA). Blotting was performed twice at 4°C with 100% relative humidity, involving three consecutive blotting steps of 3.5 seconds each with a force setting of 2. A 10 μL sample was applied to an S166 lacey carbon film 200 mesh copper grid (Agar Scientific, Stansted, UK). After blotting, the grid was plunged into liquid ethane for vitrification. The vitrified grid was then transferred to a cryo-holder (model 626, Gatan, Pleasanton, CA, USA). The samples were analysed at an accelerating voltage of 120 kV using a Tecnai F20 G² TWIN Cryo-TEM (Thermo Fisher Scientific, Waltham, MA, USA) [59].

Thermogravimetric analysis (TGA). TGA was performed on Tr-DTX, Tr-Blank and their individual constituents (DTX, oleic acid, Tween 80 and active ingredient) using the TGA Q5000IR thermal analyser (TA Instruments, USA). TGA profiles were generated with a heating rate of 10°C/min over a temperature range from room temperature to 700°C , under dynamic nitrogen atmosphere conditions (50 mL/min). The samples were placed into platinum pans (100 μL) [59, 60].

Results and Discussion

Experimental design

Based on preliminary tests examining the compatibility of the multiple edge activators and DTX, the independent variables of the Definitive Screening design were chosen. The results from the 18 evaluated formulations and the measured properties of interest (Size (nm), zeta potential – ZP (mV), Release 8 h (%), Release 24 h (%), entrapment efficiency – EE (%), Recovery (%)) are presented in Table IV. Figure 2 and Figure 3 display surface graphs depicting each statistically significant response, along with the desirability graphs (Figure 4).

Table IV

Results derived from Definitive Screening design of Tr-DTX, dependent variables (Size, ZP, Release 8 h, Release 24 h, EE and Recovery)

Formulation	Size (nm)	ZP (mV)	Release 8 h (%)	Release 24 h (%)	EE (%)	Recovery (%)
Tr_1	206.9	-13.19	121.54*	146.25*	123.12*	36.59
Tr_2	266.8	-12.78	79.80	88.78	59.73	32.16
Tr_3	550.0	-14.37	61.57	57.09	86.00	20.00
Tr_4	129.3	-5.72	66.64	75.60	50.96	67.65
Tr_5	754.5	-16.37	78.36	85.82	44.62	30.76
Tr_6	366.1	-14.37	61.48	69.38	92.74	10.99
Tr_7	646.0	-38.19	69.71	71.72	81.95	85.53
Tr_8	249.1	-13.19	48.50	50.43	38.11	76.81
Tr_9	153.3	-2.13	57.29	59.10	66.77	54.36
Tr_10	540.9	-10.65	71.89	72.22	86.40	19.08
Tr_11	65.5	-13.99	73.31	73.08	19.87	68.08
Tr_12	388.7	-14.91	47.25	55.61	89.16	14.60
Tr_13	164.9	0.00	48.93	15.31*	27.53	105.48
Tr_14	380.7	-2.13	58.60	56.24	82.73	24.47
Tr_15	75.2	-11.45	60.34	56.62	24.05	101.77
Tr_16	182.2	-6.39	64.03	65.53	77.34	37.20
Tr_17	93.2	-3.82	54.13	49.94	22.57	104.85
Tr_18	270.9	-14.32	73.62	72.88	47.63	63.03

*values not included in the model

In accordance with the results presented in Table IV, the size before filtration of DTX transfersome vesicles ranged from 65.5 to 754.5. The quantity of DTX and sonication time present the most significant effect on particle size, as shown in Figure 2a. The dimensions of transfersomes decrease with the decrease of DTX and increase of sonication time. This reduction may result from the dispersion of agglomerated vesicles into smaller ones with prolonged sonication time [61]. Also, the quantity of edge activator and its type significantly affect vesicle size (Figure 2b). The smaller dimensions are achieved when Tween 80 is used as an edge activator. The transfersomes size decreases with the rise in Tween 80 concentration. The phenomenon is attributed to the edge activator's ability to induce aggregates in excess, thereby increasing the vesicle size [62, 63]. The second-order interaction for rehydration time (E^2), as well as the interaction between rehydration time and the presence of cholesterol (EH) in the formulation, show p-values < 0.05, indicating a significant effect on vesicle size before filtration. As regards particle size after filtration, all formulations presented a vesicle size of approximately 100 nm. Therefore, this parameter was not taken into account as a criterion in model prediction and choosing the optimum formulation.

Zeta potential represents a parameter associated with the surface charge of particles, impacting the stability of colloidal [64-66]. Both decreasing rehydration volume and sonication time lead to a reduction in zeta potential. The absence of cholesterol in transfersomes formulation results in a lower zeta potential. Regarding the type of edge activator, Tween 80 leads to an increase in zeta potential as it can be observed in Figure 2c and Figure 2d. All formulations exhibited negative zeta potential, except one which had a value of 0. The electrostatic interplay between the negatively charged surface of the skin and the refined formulation could induce transient channels in the skin's structure, enhancing the drug's delivery and retention deeper into the skin layers [67-69]. Researchers suggest that negatively charged nano-carriers could enhance drug permeability and retention in transdermal delivery [70]. Hence, the negative charge of the formulations could influence the penetration of DTX transfersomes through the skin.

The amount of DTX released in 8 hours ranged between 47.25 and 79.80, while after 24 hours, the percentage of DTX released fell between 49.94 and 88.78. In both cases, the rehydration temperature had a significant effect on the release of API from the transfersomes. The higher the rehydration temperature, the higher the percentage of DTX released. Other variable contributing to rise of DTX release in time is the interaction between rehydration volume and the presence of cholesterol (DH). All these effects are presented in Figures 2e, 2f, 2g and 2h.

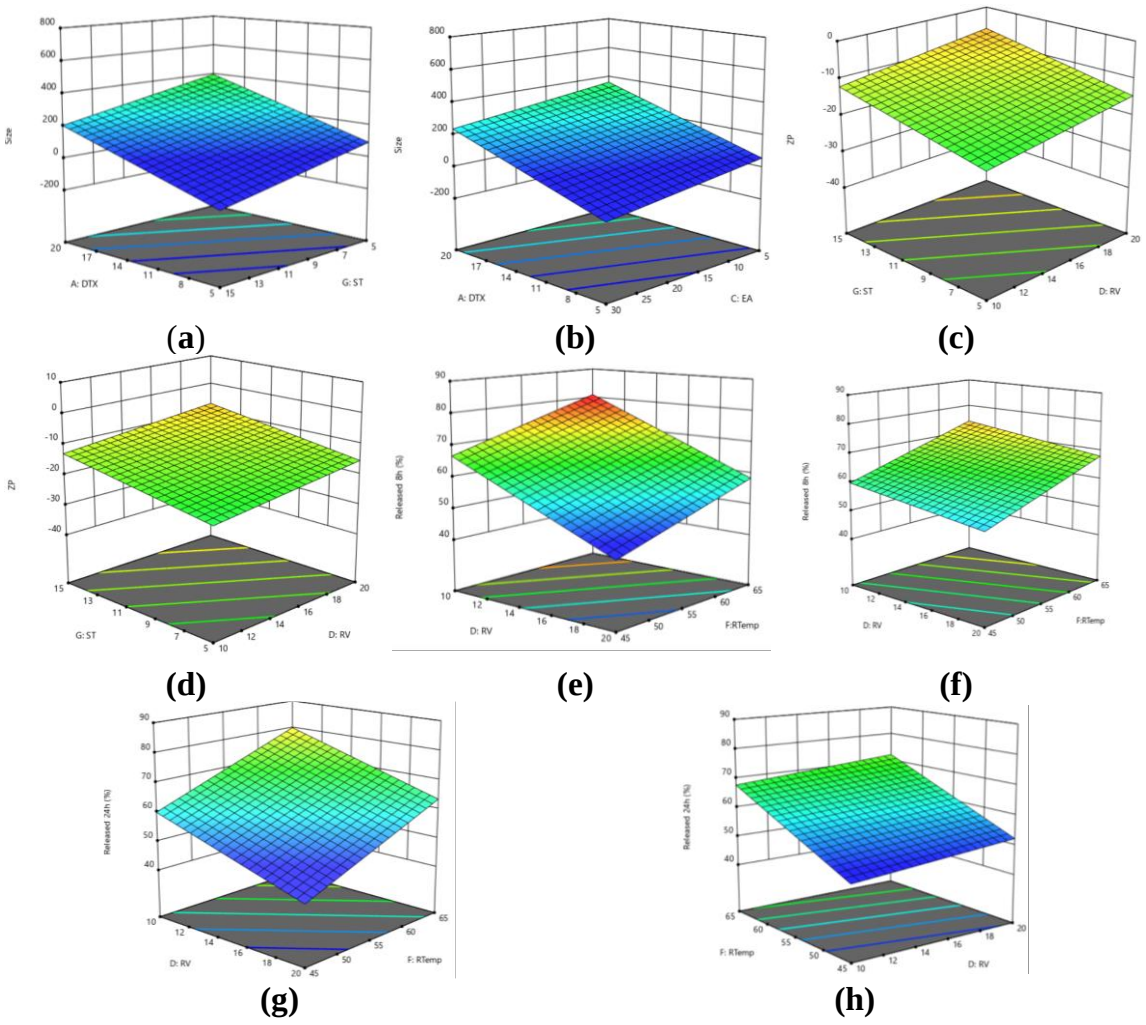

Figure 2.

Response surface for: size as a function of DTX and sonication time when T80 and Ch were used (a), size as function of DTX and quantity of EA when T80 and Ch were used (b), zeta potential as a function of rehydration volume and sonication time when T80 and Ch were used (c), zeta potential as a function of rehydration volume and sonication time when DXC was used, and Ch was absent (d), release 8 h as a function of rehydration volume and rehydration temperature when T80 and Ch were used (e), release 8 h as a function of rehydration volume and rehydration temperature when T80 was used, and Ch was absent (f), release 24 h as a function of rehydration volume and rehydration temperature when T80 and Ch were used (g), release 24 h as a function of rehydration volume and rehydration temperature when T80 was used and Ch was absent (h)

The amount of DTX entrapped in transfersomes is highly influenced by the amount of API, rehydration time, the interactions between DTX and quantity of edge activator (AC), DTX and sonication time (AG), quantity of edge activator and rehydration time (CE), respectively second interaction of amount of edge activator (C2). The type of edge activator or the presence of cholesterol in formulation does not influence the entrapment efficiency. All these interactions are also represented in Figures 3a, 3b, 3c and 3d.

The percentage of DTX recovered after filtration (Recovery (%)) represents one of the most important dependent variables analysed in DoE. It is closely correlated with entrapment efficiency. The independent variables contributing to the increase of recovery were the amount of DTX, the type of edge activator, rehydration temperature, interactions between DTX and quantity of edge activator (AC), and type of edge activator and sonication time (BG). The lowest the amount of DTX, the higher the recovery after filtration. The impact of each mentioned independent variable and interaction is better illustrated through response surfaces represented in Figures 3e, 3f, 3g and 3h.

Following the testing of DTX solutions maintained for two hours at the rehydration temperatures tested in DoE, it was observed that with the increase in temperature from 45°C to 65°C, the amount of DTX decreased while the quantity of impurities increased. This outcome can be corelated with the slow recovery in DTX for all the formulations rehydrated at temperatures higher than 50°C.

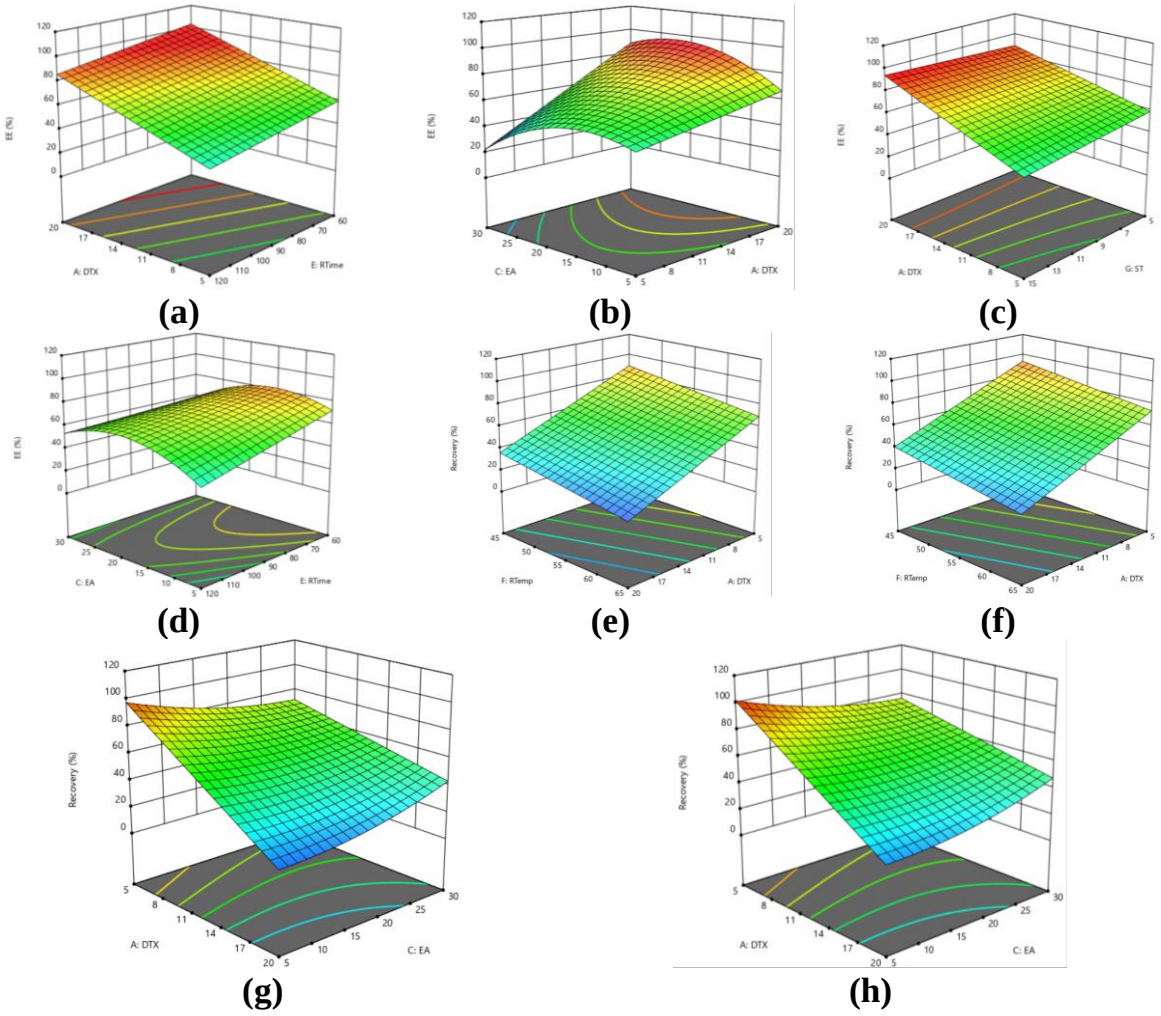

Figure 3.

Response surface for: entrapment efficiency as a function of DTX and rehydration time when T80 and Ch were used (a), entrapment efficiency as a function of DTX and quantity of EA when T80 and Ch were used (b), entrapment efficiency as a function of DTX and sonication time when T80 and Ch were used (c), entrapment efficiency as a function of the quantity of EA and rehydration time when T80 and Ch were used (d), recovery as a function of DTX and rehydration temperature when T80 and Ch were used (e), recovery as a function of DTX and rehydration temperature when DXC and Ch were used (f), recovery as a function of DTX and quantity of EA when T80 and Ch were used (g), recovery as a function of DTX and quantity of EA when DXC and Ch were used (h)

By applying predetermined criteria (including lower size, higher release at 8 hours, respectively at 24 hours, higher entrapment efficiency and high recovery after filtration), a desirability graph was generated (Figure 4), where the desirability parameter directly indicates the degree of alignment of the formulation with the established criteria (a value close to 1 indicates better alignment). In the case of Tr-DTX, the desirability value of 0.787 signalled those conditions closer to a corner point yielded a more favourable correspondence with the desired criteria. Consequently, the best overall answer (BOA) obtained from the screening design consists of 20 mg DTX, Tween 80 as edge activator, 30 mg of edge activator, rehydration with 10 mL of phosphate buffer for 90 minutes at 50°C, and sonication.

One-Factor-at-a-Time (OFAT)

Expanding on the optimal outcome derived from the screening design, OFAT experiments were conducted. The first formulation tested was BOA when the precipitation phenomenon was observed. This indicates that the amount of DTX is too high for the entrapment efficacy of the phospholipidic structure. Then, the quantity of DTX was optimised (F2 - F4). Since cholesterol confers stiffness to the vesicles, the incorporation of a liquid lipid (oleic acid) was tested (F5) to enhance their deformability, thereby facilitating penetration into the deeper layers of the skin, even leading to its exclusion from formulations. All the variations and the results are presented in Table III.

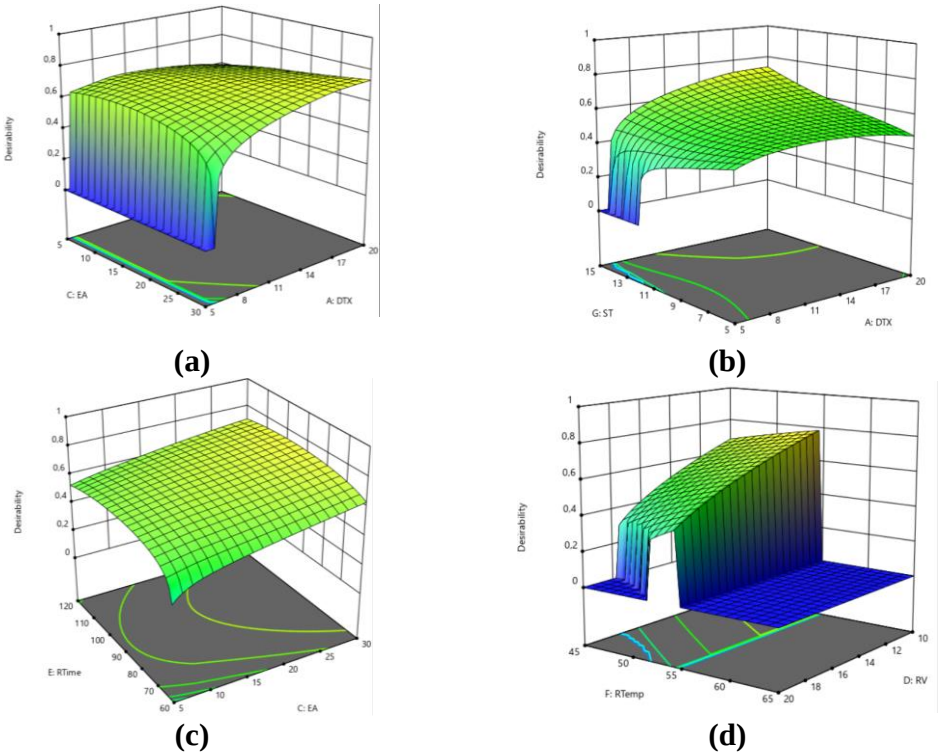

Figure 4.

Response surface as a function of: DTX and quantity of EA when T80 and Ch were used (a), DTX and sonication time when T80 and Ch were used (b), the quantity of EA and rehydration time when T80 and Ch were used (c), rehydration volume and rehydration temperature when T80 and Ch were used (d)

From the presented data, it can be observed that replacing cholesterol with oleic acid leads to a decrease in zeta potential, indicating better stability of the formed system and an increase in recovery, indicating better entrapment of the API. From the literature data presented, cholesterol is known to have the ability to form rigid bilayer structures together with phosphatidyl-choline [71-73]. However, when the site of drug delivery is deep within the skin, it is desirable for vesicles to be more flexible and easily deformable. In this context, cholesterol can be replaced with liquid lipids such as oleic acid. Moreover, this one also exhibits edge activator properties [74, 75]. Also, it is known that oleic acid can increase the stability of the bilayers formed [76, 77]. The addition of oleic acid in the formulation was conducted to achieve greater recovery, entrapment efficiency and lower zeta potential. The percentage of DTX recovered after filtration is one of the most crucial dependent variables analysed in both types of experiments, closely linked to entrapment efficiency and *in vitro* release of API from the matrix. The higher the recovery after filtration, the higher the encapsulation efficiency and percentage of DTX release over time. Independent variables contributing to an increase in recovery include the amount of DTX, the type and quantity of edge activator, rehydration temperature, sonication time and their interactions.

As a result, the chosen formulation consisted of 12.5 mg DTX, 20 mg Tween 80, 20 mg oleic acid, and rehydration with 10 mL of phosphate buffer for 90 minutes at 50°C. Subsequently, both the optimized formulation and the control sample (manufactured without DTX) were prepared in triplicate, and their characterisation was conducted.

Characterisation of the optimised transfersomes formulation

Size, PDI, zeta potential and entrapment efficiency

The optimised formulations (Tr-DTX) along with the control counterpart (Tr-Blank), formulated without DTX, were characterised, and their physicochemical properties are outlined in Table V.

Table V

Physicochemical properties (size, PDI, ZP, EE %, Recovery %) of the Tr-DTX formulation selected by the Definitive Screening design and OFAT experiments and its control

Formulation	Size (nm)	PDI	ZP (mV)	EE %	Recovery %	Release 8 h	Release 24 h
Tr-DTX	96.63 ± 5.14	0.2090 ± 0.0452	-15.97 ± 1.60	75.87 ± 4.13	97.51 ± 4.04	50.11 ± 6.60	79.51 ± 2.04
Tr-Blank	86.6 ± 2.40	0.2847 ± 0.0270	-6.92 ± 0.06	-	-	-	-

The particle size of Tr-DTX exhibits a slight increase compared to Tr-Blank. It is noteworthy that there were no differences between the three replicates regarding this control parameter. Despite the slight increase in transfersomal size due to DTX addition, both sample types displayed consistently low PDI values (< 0.3), indicating uniform size distribution [78, 79]. Additionally, the zeta potential values deviated significantly from the neutrality, which is favourable for long-term stability in pharmaceutical formulations [30, 64-66, 80].

Morphology imaging

The particle size can be confirmed using an orthogonal microscopy technique, such as SEM and Cryo-TEM, which can also illustrate their morphology.

As expected for lipid carriers such as these, both formulations, with and without DTX, predominantly exhibited spherical particles with smooth surfaces (Figure 5a and Figure 5b). The Cryo-TEM high-resolution micrographs distinctly show the bilayer structure of the transfersomes, indicating successful formulation. The images also demonstrate that the transfersomes maintain their structural integrity without aggregation, confirming the stability of the formulation (Figure 5c and Figure 5d). The observed vesicles present a size of approximately 100 nm, consistent with the dynamic light scattering results (Figure 5d). Importantly, the incorporation of DTX into the system did not induce any alteration to the transfersomes morphology.

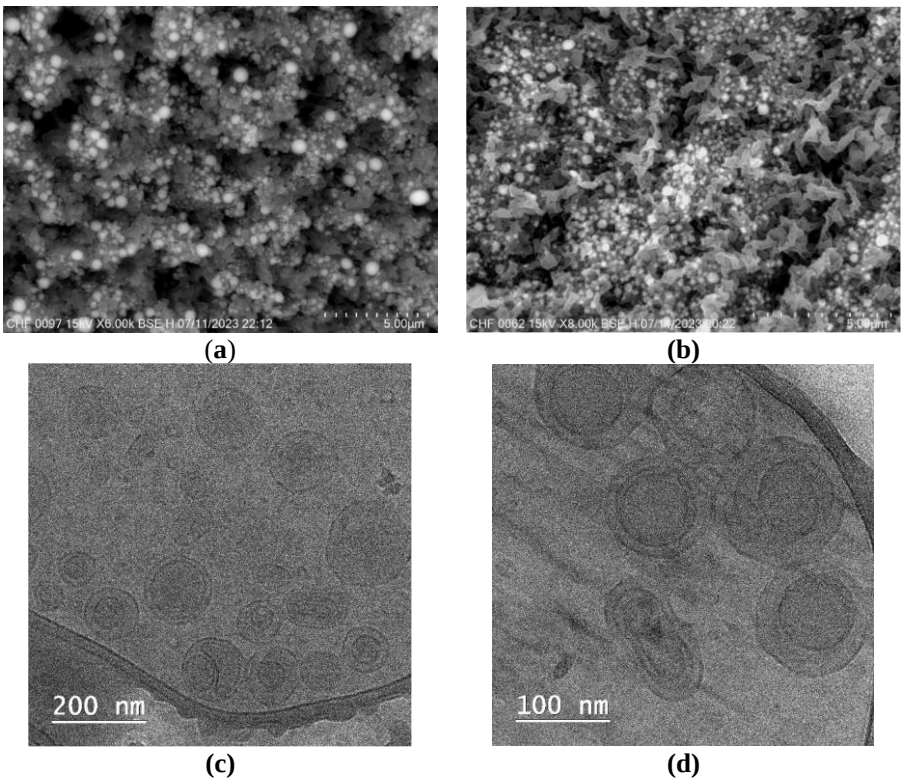

Figure 5.
SEM micrographs of the optimised formulations Tr-Blank (a), respectively Tr-DTX (b), Cryo - TEM micrographs of the optimised formulation at different scales: 200nm (c), 100 nm (d)

Thermal analysis

All the excipients which form the lipid film, DTX, the blank formulation and the loaded one underwent to thermogravimetric analysis (TGA).

DTX exhibits thermal stability up to roughly 120°C, as indicated by a minimal mass reduction of 0.35%, primarily attributed to the release of incorporated water. Beyond this temperature threshold, thermal decomposition proceeds through two distinct phases. The initial phase spans from approximately 120°C to 320°C, resulting in a mass loss of 56.48%. This is followed by a secondary phase extending from about 320°C to 560°C, accompanied by a mass loss of 26.70%. Subsequent analysis unveiled a residual mass of 16.53%. Additionally, the decomposition process is characterised by two notable peaks in derived weight (%/min) observed at 205°C and 343°C, respectively.

Regarding the excipients, oleic acid (AO) and Tween 80 (T80) present thermal decomposition in only one phase, namely between 120°C and 300°C with a mass loss of 98.14% for oleic acid, respectively between 300°C and 500°C with a mass loss of 95.51% for Tween 80. Both excipients present only one peak in the derived weighed (%/min), oleic acid at 240°C and Tween 80 at 403°C, respectively. Phospholipon

90G, owing to its diverse composition, undergoes decomposition within the tested temperature range in multiple stages as follows: up to 180°C it loses 5.08% mass, between 180°C and 250°C 5.74%, continuing to loss 39.96% up to 320°C, from this temperature to 390°C it loses 32.41%, between 390°C and 530°C it presents a mass loss of 7.43%, in the last stage loses 1.31% up to 700°C. At the end of the analysis, a residue of 8.07% was found.

Both the blank formulation (Tr-Blank) and the formulation containing DTX (Tr-DTX) exhibit similar thermal behaviours, with each presenting four discernible stages: initially, a decrease of 5.14% in mass for Tr-Blank and 4.21% in mass for Tr-DTX up to around 150°C, attributed to water content; followed by a second phase spanning approximately 150°C to 190°C, resulting in mass losses of 1.47% for Tr-Blank and 1.50% for Tr-DTX, respectively. The third stage extends until about 340°C, with mass losses of 71.80% for Tr-Blank and 68.85% for Tr-DTX. In the final stage, up to 700°C, the blank formulation experiences a loss of 8.84%, while the Tr with DTX loses 10.81%. Also, at the end of the analysis, Tr-Blank presented 13.68% residue, while Tr-DTX had 13.70% residue. Both formulations' decomposition processes are characterised by two primary peaks in derived weight (%/min), at 290°C, respectively at 357°C.

Figure 6 presents the TGA analysis results, comparing Tr-Blank, Tr-DTX, DTX and excipients, highlighting the differences in thermal behaviour among the excipients, API and formulations, and the similarities between the two transfersomal formulations tested.

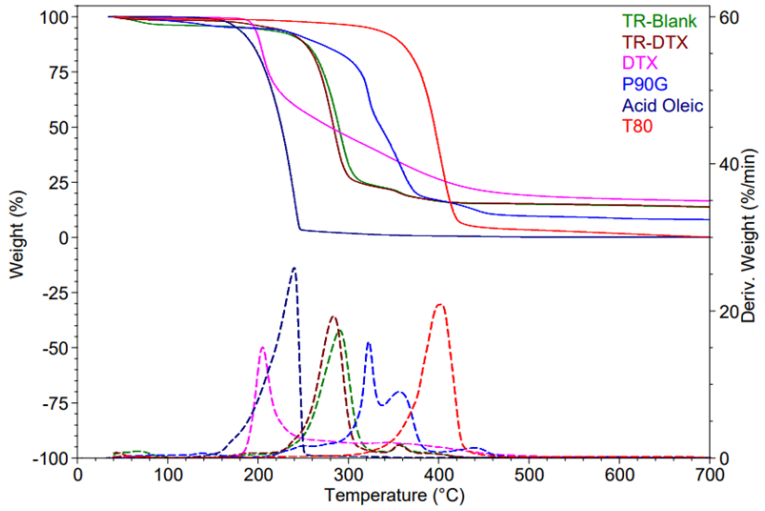

Figure 6.
Thermograms of excipients, DTX and formulations (Tr-Blank and Tr-DTX)

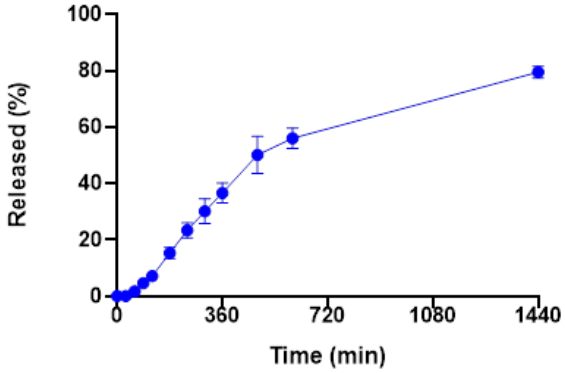

Figure 7.
In vitro release profile for encapsulated active ingredient determined at 37°C, receptor medium composed of PBS: ethanol (80:20, v/v), n = 6

In vitro release kinetics

Figure 7 illustrates the outcomes regarding the *in vitro* release kinetics of DTX encapsulated within the optimised transfersomes formulation. It is evident that around 80% of DTX was released within 24 hours, which is observed as a sustained release of the API. Interestingly, the formulation did not display an initial burst release phase, likely attributable to the higher encapsulation of the drug (EE = 75%) with the transfersomes.

Various mathematical models have been employed to characterise the release patterns of lipid, polymer and lipid-polymer drug delivery systems containing different APIs [62, 81-83]. To gain a deeper insight into the mechanisms governing DTX release, the data depicted in Figure 8 underwent fitting using several kinetic models. The most appropriate fits for Tr-DTX kinetics were achieved with the Higuchi (R^2 = 0.9820) and Noyes-Whitney (first-order kinetics) (R^2 = 0.9860). The Higuchi model suggests that the solvent gradually causes the matrix to swell and describes the concentration gradient as linear, decreasing from the saturation concentration at the interface with the core, which is not exposed to the solvent, to a concentration of zero (sink conditions) at the interface between the matrix and the dissolution medium [83]. The principle of first-order release suggests that the

rate of release kinetics is contingent upon the alteration of drug concentration over time. The highest R^2 value achieved for the Noyes Whitney model implies that changes in drug release rate and kinetics were influenced by the concentration of DTX.

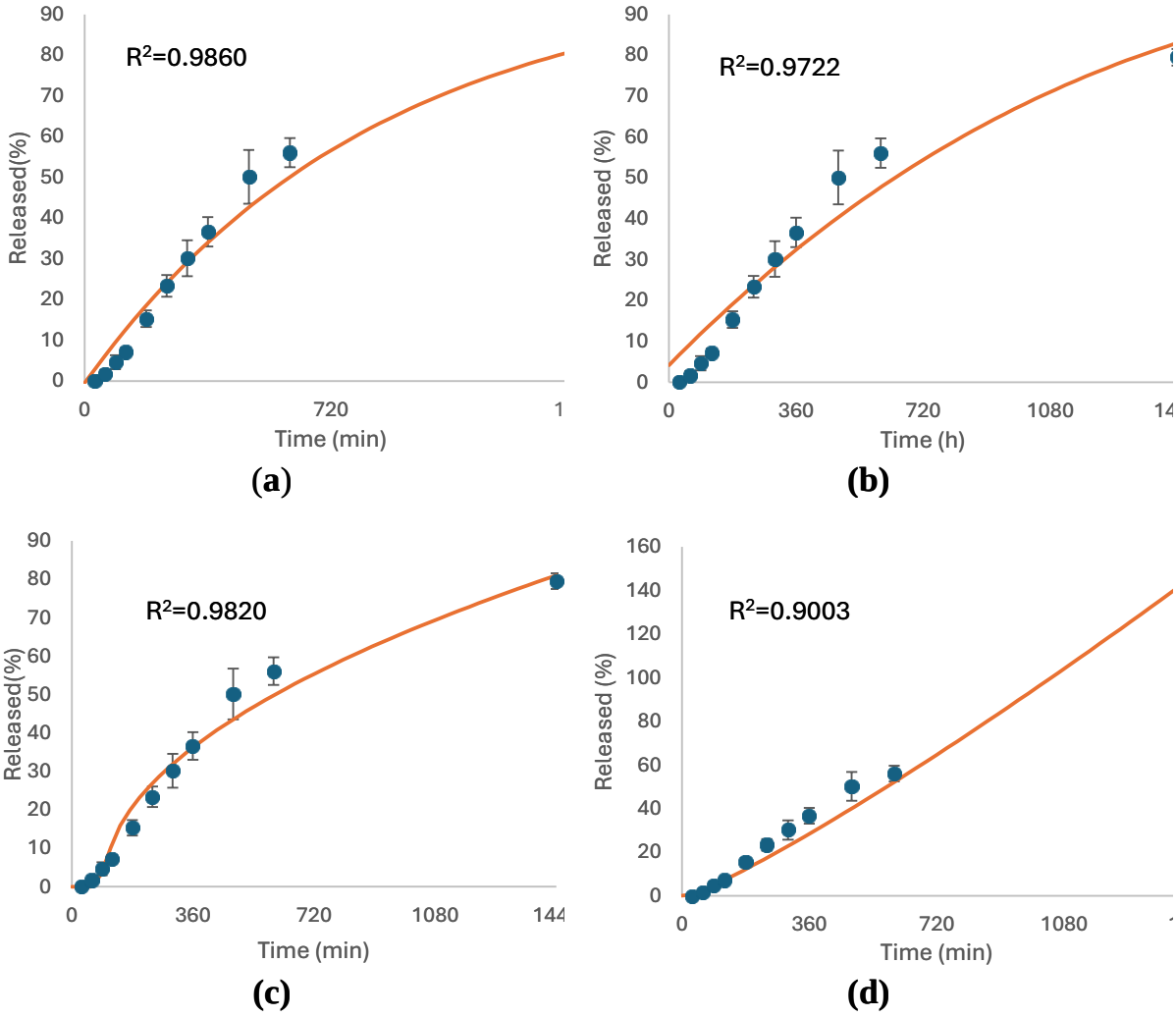

Figure 8.
In vitro release kinetics (a) Noyes-Whitney model, (b) Hixson-Crowell model, (c) Higuchi model and (d) Korsmeyer-Peppas model

Conclusions

Through a comprehensive investigation encompassing Design of Experiments (DoE) and One-Factor-at-a-Time (OFAT) experiments, we systematically optimised the formulation parameters for active ingredient-loaded transfersomes. Our findings revealed significant influences of several factors on the physicochemical properties of transfersomes, including particle size, zeta potential, encapsulation efficiency and recovery.Notably, selecting an optimised formulation comprising specific quantities of AI, edge activators and rehydration conditions was pivotal in achieving desirable characteristics. Characterisation studies confirmed the consistent particle size distribution and morphology of transfersomes, underscoring their suitability for therapeutic applications. Furthermore, *in vitro* release kinetics studies elucidated sustained drug release profiles, indicative of the potential for prolonged therapeutic efficacy.

This study underscores the promise of transfersomes as a viable approach for localized drug delivery in skin cancer treatment, aiming to improve therapeutic outcomes and patient safety.

Acknowledgement

A part of this research was supported by "Carol Davila" University of Medicine and Pharmacy, Bucharest, Romania through Contract no. 33PFE/ 30.12.2021 and Contract CNFIS-FDI-2024-F-0570.

Conflict of interest

The authors declare no conflict of interest.

References

1. da Rocha MCO, da Silva PB, Radicchi MA, Andrade BYG, de Oliveira JV, Venus T, Merker C, Estrela-Lopis I, Longo JPF, Báo SN, active ingredient-loaded solid lipid nanoparticles prevent tumor growth and lung metastasis of 4T1 murine mammary carcinoma cells. *J Nanobiotechnol.*, 2020; 18(1): 43.
2. Cho HJ, Park JW, Yoon IS, Kim DD, Surface-modified solid lipid nanoparticles for oral delivery of active ingredient: enhanced intestinal absorption and lymphatic uptake. *Int J Nanomed.*, 2014; 9: 495-504.
3. Thambiraj S, Vijayalakshmi R, Ravi Shankaran D, An effective strategy for development of active ingredient encapsulated gold nanoformulations for treatment of prostate cancer. *Sci Rep.*, 2021; 11(1): 2808.
4. Popa CN, Bîrlă RD, Dinu DE, Iosif C, Bogaseriu E, Mateș IN, Breast cancer response to neoadjuvant chemotherapy quantified by residual cancer burden (RCB) score. *Farmacia*, 2022; 70(4): 712-719.
5. www.Accessdata.Fda.Gov/Scripts/Cder/Daf/Index.Cfm?Event=BasicSearch.Process.
6. Ciobanu AE, Pîrvu DC, Mărginean CM, Dijmărescu AL, Muñoz-Groza AE, Meșină C, Bălșeanu TA, Băleanu VD, Țenea-Cojan TȘ, Ciobanu D, Molecular prognostic factors in colorectal cancer: 5-year follow-up. *Rom J Morphol Embryol.*, 2023; 64(1): 65-71.
7. www.Ema.Europa.Eu/En/Medicines/Human/EPAR/Active Ingredient.
8. Fang G, Tang B, Chao Y, Xu H, Gou J, Zhang Y, Xu H, Tang X, Cysteine-Functionalized Nanostructured Lipid Carriers for Oral Delivery of active ingredient: A Permeability and Pharmacokinetic Study. *Mol Pharm.*,2015; 12(7): 2384-2395.
9. Park MH, Keum CG, Song JY, Kim D, Cho CW, A novel aqueous parenteral formulation of active ingredient using prodrugs. *Int J Pharm.*, 2014; 462 (1-2): 1-7.
10. Engels F, Mathot R, Verweij J, Alternative drug formulations of active ingredient: A review. *Anti-cancer Drugs*, 2007; 18: 95-103.
11. Seo YG, Kim DW, Yeo WH, Ramasamy T, Oh YK, Park YJ, Kim JA, Oh DH, Ku SK, Kim JK, Yong CS, Kim JO, Choi HG, active ingredient-loaded thermosensitive and bioadhesive nanomicelles as a rectal drug delivery system for enhanced chemotherapeutic effect. *Pharm Res.*, 2013; 30(7): 1860-1870.
12. Tan Q, Liu X, Fu X, Li Q, Dou J, Zhai G, Current development in nanoformulations of active ingredient. *Expert Opin Drug Deliv.*, 2012; 9(8): 975-990.
13. Schwartzberg LS, Navari RM, Safety of Polysorbate 80 in the Oncology Setting. *Adv Ther.*, 2018; 35(6): 754-767.
14. ten Tije AJ, Verweij J, Loos WJ, Sparreboom A, Pharmacological effects of formulation vehicles: implications for cancer chemotherapy. *Clin Pharmacok.*, 2003; 42(7): 665-685.
15. Brannon-Peppas L, Blanchette JO, Nanoparticle and targeted systems for cancer therapy. *Adv Drug Deliv Rev.*, 2004; 56(11): 1649-1659.
16. Predut D, Semenescu AD, Manea A, Dinu S, Popovici R, Jivanescu A, Cytotoxicity assessment of liposomes loaded with biologically active substances on oral tumour cells. *Farmacia*, 2022; 70(6): 1081-1088.
17. Muthu MS, Kulkarni SA, Xiong J, Feng SS, Vitamin E TPGS coated liposomes enhanced cellular uptake and cytotoxicity of active ingredient in brain cancer cells. *Int J Pharm.*, 2011; 421(2): 332-340.
18. Li X, Tian X, Zhang J, Zhao X, Chen X, Jiang Y, Wang D, Pan W, *In vitro* and *in vivo* evaluation of folate receptor-targeting amphiphilic copolymer-modified liposomes loaded with active ingredient *Int J Nanomed.*, 2011; 6: 1167-1184.
19. Zhai G, Wu J, Yu B, Guo C, Yang X, Lee R, A Transferrin Receptor-Targeted Liposomal Formulation for Active Ingredient. *J Nanosci Nanotechn.*, 2010; 10: 5129-5136.
20. Xu Z, Chen L, Gu W, Gao Y, Lin L, Zhang Z, Xi Y, Li Y, The performance of active ingredient-loaded solid lipid nanoparticles targeted to hepatocellular carcinoma. *Biomaterials*, 2009; 30(2): 226-232.
21. Kharkar PB, Talkar SS, Patravale VB, An industrially viable technique for fabrication of active ingredient NLCs for oncotherapy. *Int J Pharm.*, 2020; 577: 119082.
22. Liu D, Liu F, Liu Z, Wang L, Zhang N, Tumour specific delivery and therapy by double-targeted nanostructured lipid carriers with anti-VEGFR-2 antibody. *Mol Pharm.*, 2011; 8(6): 2291-2301.
23. Hua H, Zhang N, Liu D, Song L, Liu T, Li S, Zhao Y, Multifunctional gold nanorods and active ingredient-encapsulated liposomes for combined thermo- and chemotherapy. *Int J Nanomed.*, 2017; 12(null): 7869-7884.
24. Khan MA, Pandit J, Sultana Y, Sultana S, Ali A, Aqil M, Chauhan M, Novel carbopol-based transfersomal gel of 5-active ingredient for skin cancer treatment: *in vitro* characterization and *in vivo* study. *Drug Deliv.*, 2015; 22(6): 795-802.
25. Opatha SAT, Titapiwatanakun V, Chutoprapat R, Transfersomes: A Promising Nanoencapsulation Technique for Transdermal Drug Delivery. *Pharmaceutics*, 2020; 12(9): 855.
26. Chen M, Shamim MA, Shahid A, Yeung S, Andresen BT, Wang J, Nekkanti V, Meyskens FL Jr, Kelly KM, Huang Y, Topical Delivery of active ingredeint Loaded Nano-Transfersomes for Skin Cancer Chemoprevention .*Pharmaceutics*, 2020; 12(12): 1151.
27. Rai S, Pandey V, Rai G, Transfersomes as versatile and flexible nano-vesicular carriers in skin cancer therapy: the state of the art. *Nano Rev Exper.*, 2017; 8(1): 1325708.
28. Opatha SAT, Titapiwatanakun V, Boonpisutiinant K, Chutoprapat R, Preparation, Characterization and Permeation Study of Topical Gel Loaded with Transfersomes Containing Asiatic Acid. *Molecules*, 2022; 27(15): 4865.
29. Jiang T, Wang T, Li T, Ma Y, Shen S, He B, Mo R, Enhanced Transdermal Drug Delivery by Transfersome-Embedded Oligopeptide Hydrogel for Topical Chemotherapy of Melanoma. *ACS Nano*, 2018; 12(10): 9693-9701.
30. Garg V, Singh H, Bimbrawh S, Singh SK, Gulati M, Vaidya Y, Kaur P, Ethosomes and Transfersomes: Principles, Perspectives and Practices. *Curr Drug Deliv.*, 2017; 14(5): 613-633.
31. Kotla NG, Chandrasekar B, Rooney P, Sivaraman G, Larranaga A, Vijaya Krishna K, Pandit A, Rochev Y, Biomimetic Lipid-Based Nanosystems for Enhanced

Dermal Delivery of Drugs and Bioactive Agents. *ACS Biomater Sci Eng*.. 2017; 3(7): 1262-1272.
32. Kotla NG, Chandrasekar B, Rooney P, Sivaraman G, Larrañaga A, Krishna KV, Pandit A, Rochev Y, Development, characterization, and skin delivery studies of related ultradeformable vesicles: transfersomes, ethosomes, and transethosomes. *Int J Nanomed*., 2015; 10: 5837-5851.
33. Leonyza A, Surini S, Optimization of Sodium Deoxycholate-Based Transfersomes for Percutaneous Delivery of Peptides and Proteins. *Int J Appl Pharm*., 2019; 11(5): 329-332.
34. Cevc G, Transdermal drug delivery of active ingredient with ultradeformable carriers. *Clin Pharmacokinet*., 2003; 42(5): 461-474.
35. Cevc G, Gebauer D, Stieber J, Schätzlein A, Blume G, Ultraflexible vesicles, Transfersomes, have an extremely low pore penetration resistance and transport therapeutic amounts of active ingredient across the intact mammalian skin. *Biochim Biophys Acta* , 1998; 1368(2): 201-215.
36. Cevc G, Blume G, Hydrocortisone and active ingredient in very deformable drug carriers have increased biological potency, prolonged effect, and reduced therapeutic dosage. *Biochim Biophys Acta*, 2004; 1663(1-2): 61-73.
37. Cevc G, Blume G, Biological activity and characteristics of active ingredient-acetonide formulated with the self-regulating drug carriers, Transfersomes . *Biochim Biophys Acta*, 2003; 1614(2): 156-164.
38. Cevc G, Blume G, Schätzlein A, Transfersomes-mediated transepidermal delivery improves the regio-specificity and biological activity of corticosteroids *in vivo*. *J Control Rel.*, 1997; 45(3): 211-226.
39. Bnyan R, Khan I, Ehtezazi T, Saleem I, Gordon S, O'Neill F, Roberts M, Formulation and optimisation of novel transfersomes for sustained release of local anaesthetic. *J Pharm Pharmacol.*, 2019; 71(10): 1508-1519.
40. Omar MM, Hasan OA, El Sisi AM, Preparation and optimization of lidocaine transferosomal gel containing permeation enhancers: a promising approach for enhancement of skin permeation. *Int J Nanomed.*, 2019; 14: 1551-1562.
41. Rother M, Lavins BJ, Kneer W, Lehnhardt K, Seidel EJ, Efficacy and safety of epicutaneous active ingredient in Transfersome (IDEA-033) *versus* oral active ingredient and placebo in osteoarthritis of the knee: multicentre randomised controlled trial. *Ann Rheum Dis.*, 2007; 66(9): 1178-1183.
42. Duangjit S, Opanasopit P, Rojanarata T, Ngawhirunpat T, Characterization and *In Vitro* Skin Permeation of active ingredient-Loaded Liposomes *versus* Transfersomes.*J Drug Deliv.*, 2011; 2011: 418316.
43. Irfan M, Verma S, Ram A, Preparation and characterization of Ibuprofen loaded transferosome as a novel carrier for transdermal drug delivery system. *Asian J Pharm Clin Res.*, 2012; 5: 162-165.
44. Modi C, Bharadia PD, Transfersomes: New Dominants for Transdermal Drug Delivery. *Am J PharmTech Res.*, 2012; 2(3): 71-91.
45. Lu WL, Qi XR, Liposome-based drug delivery systems: Springer; 2021.
46. Sciolla F, Truzzolillo D, Chauveau E, Trabalzini S, Di Marzio L, Carafa M, Marianecci C, Sarra A, Bordi F, Sennato S, Influence of drug/lipid interaction on the entrapment efficiency of AI in liposomes for antitubercular therapy: a multi-faced investigation. *Colloids Surf B Biointerfaces*, 2021; 208: 112054.
47. Delama A, Teixeira MI, Dorati R, Genta I, Conti B, Lamprou DA, Microfluidic encapsulation method to produce stable liposomes containing active ingredient. *J DrugDeliv Sci Techn.*, 2019; 54:101340.
48. Slavkova M, Tzankov B, Popova T, Voycheva C, Gel Formulations for Topical Treatment of Skin Cancer: A Review. *Gels*, 2023; 9(5): 352.
49. Yue PF, Lu XY, Zhang ZZ, Yuan HL, Zhu WF, Zheng Q, Yang M, The study on the entrapment efficiency and *in vitro* release of puerarin submicron emulsion. *AAPS PharmSciTech.*, 2009; 10(2): 376-383.
50. Moyá ML, López-López M, Lebrón JA, Ostos FJ, Pérez D, Camacho V, Beck I, Merino-Bohórquez V, Camean M, Madinabeitia N, López-Cornejo P, Preparation and Characterization of New Liposomes. Bactericidal Activity of AI Encapsulated into Cationic Liposomes. *Pharmaceutics*, 2019; 11(2): 69.
51. Uwaezuoke O, Du Toit LC, Kumar P, Ally N, Choonara YE, Linoleic Acid-Based Transferosomes for Topical Ocular Delivery of active ingredient A. *Pharmaceutics*, 2022; 14(8): 1695.
52. Barbalata CI, Porfire AS, Casian T, Muntean D, Rus I, Tertis M, Cristea C, Pop A, Cherfan J, Loghin F, Tomuta I, The Use of the QbD Approach to Optimize the Co-Loading of active ingredient and AI in Liposomes for a Synergistic Anticancer Effect. *Pharmaceuticals*, 2022; 15(10): 1211.
53. Barbălată CI, Porfire AS, Sesarman A, Rauca VF, Banciu M, Muntean D, Știufiuc R, Moldovan A, Moldovan C, Tomuță I, A Screening Study for the Development of active ingredient Liposomes, a Co-Formulation with Future Perspectives in Colon Cancer Therapy.*Pharmaceutics*, 2021; 13(10): 1526.54. Bao Q, Wang X, Zou Y, Wang Y, Burgess DJ, *In vitro* release testing method development for long-acting injectable suspensions. *Int J Pharm.*, 2022; 622: 121840.
55. Rawat A, Burgess DJ, USP apparatus 4 method for *in vitro* release testing of protein loaded microspheres. *Int J Pharm.*, 2011; 409(1-2): 178-184.
56. Németh Z, Csóka I, Semnani Jazani R, Sipos B, Haspel H, Kozma G, Kónya Z, Dobó DG, Quality by Design-Driven Zeta Potential Optimisation Study of Liposomes with Charge Imparting Membrane Additives. *Pharmaceutics*, 2022; 14(9): 1798.
57. Nojoki F, Ebrahimi-Hosseinzadeh B, Hatamian-Zarmi A, Khodagholi F, Khezri K, Design and development of chitosan-active ingredient-transfersomes (Transfersulin) as effective intranasal nanovesicles for the treatment of Alzheimer's disease: *In vitro*, *in vivo*, and *ex vivo* evaluations. *Biomed Pharmacother.* , 2022; 153: 113450.
58. Moqejwa T, Marimuthu T, Kondiah PPD, Choonara YE, Development of Stable Nano-Sized Transfersomes as a Rectal Colloid for Enhanced Delivery of Cannabidiol. *Pharmaceutics*, 2022; 14(4): 703.
59. Scioli-Montoto S, Sbaraglini ML, Cisneros JS, Chain CY, Ferretti V, León IE, Alvarez VA, Castro GR, Islan GA, Talevi A, Novel Phenobarbital-Loaded

Nanostructured Lipid Carriers for Epilepsy Treatment: From QbD to *In Vivo* Evaluation. *Front Chem.*, 2022; 10: 908386.
60. Losito DW, Lopes PS, Ueoka AR, Fantini MCA, Oseliero Filho PL, Andréo-Filho N, Martins TS, Biocomposites based on SBA-15 and papain: Characterization, enzymatic activity and cytotoxicity evaluation. *Microporous Mesoporous Mater.*, 2021; 325: 111316.
61. He Y, Luo L, Liang S, Long M, Xu H, Influence of probe-sonication process on drug entrapment efficiency of liposomes loaded with a hydrophobic drug. *Int J Polym Mat Polym Biomat.*, 2018; 68(4): 193-197.
62. Ghazwani M, Alqarni MH, Hani U, Alam A, QbD-Optimized, Phospholipid-Based Elastic Nanovesicles for the Effective Delivery of 6-Gingerol: A Promising Topical Option for Pain-Related Disorders. *Int J Mol Sci.*, 2023; 24(12): 9983.
63. Kazmi I, Al-Abbasi FA, Nadeem MS, Altayb HN, Alshehri S, Imam SS, Formulation, Optimization and Evaluation of Luteolin-Loaded Topical Nanoparticulate Delivery System for the Skin Cancer. *Pharmaceutics*, 2021; 13(11): 1749.
64. Elsewedy HS, Shehata TM, Almostafa MM, Soliman WE, Hypolipidemic Activity of Olive Oil-Based Nanostructured Lipid Carrier Containing active ingredient. *Nanomaterials*, 2022; 12(13): 2160.
65. Gundogdu E, Demir ES, Ekinci M, Ozgenc E, Ilem-Ozdemir D, Senyigit Z, Gonzalez-Alvarez I, Bermejo M, An Innovative Formulation Based on Nanostructured Lipid Carriers for active ingredient Delivery:Pre-Formulation, Cellular Uptake and Cytotoxicity Studies. *Nanomaterials*, 2022; 12(2): 250.
66. Kumar A, Dixit CK, Methods for characterization of nanoparticles. In: Nimesh S, Chandra R, Gupta N, editors. Advances in Nanomedicine for the Delivery of Therapeutic Nucleic Acids. Woodhead Publishing; 2017; 43-58.
67. Kammoun AK, Khedr A, Hegazy MA, Almalki AJ, Hosny KM, Abualsunun WA, Murshid SSA, Bakhaidar RB, Formulation, optimization, and nephrotoxicity evaluation of an antifungal *in situ* nasal gel loaded with active ingredient–clove oil transferosomal nanoparticles. *Drug Deliv.*, 2021; 28(1): 2229-2240.
68. Malakar J, Sen SO, Nayak AK, Sen KK, Formulation, optimization and evaluation of transferosomal gel for transdermal active ingredient delivery. *Saudi Pharm J.*, 2012; 20(4): 355-363.
69. Maione-Silva L, de Castro EG, Nascimento TL, Cintra ER, Moreira LC, Cintra BAS, Valadares MC, Lima EM, Ascorbic acid encapsulated into negatively charged liposomes exhibits increased skin permeation, retention and enhances collagen synthesis by fibroblasts. *Sci Rep.*, 2019; 9(1): 522.
70. Dudhipala N, Phasha Mohammed R, Adel Ali Youssef A, Banala N, Effect of lipid and edge activator concentration on development of aceclofenac-loaded transfersomes gel for transdermal application: *in vitro* and *ex vivo* skin permeation. *Drug Develop Industr Pharm.*, 2020; 46(8): 1334-1344.
71. Kurniawan J, Suga K, Kuhl TL, Interaction forces and membrane charge tunability: Oleic acid containing membranes in different pH conditions. *Biochim Biophys Acta Biomembr.*, 2017; 1859(2): 211-217.
72. Shaker S, Gardouh AR, Ghorab MM, Factors affecting liposomes particle size prepared by ethanol injection method. *Res Pharm Sci.*, 2017; 12(5): 346-352.
73. Şahin Bektay H, Kahraman E, Güngör S, Design of skin-simulating nanoformulations for ceramide replacement in the skin: a preliminary study. *Maced Pharm Bull.*, 2020; 66(03): 101-102.
74. Sahin Bektay H, Sagiroglu AA, Bozali K, Guler EM, Gungor S, The Design and Optimization of Ceramide NP-Loaded Liposomes to Restore the Skin Barrier. *Pharmaceutics*, 2023; 15(12): 2685.
75. Kim DH, An EJ, Kim J, Han SH, Kim JW, Oh SG, Suh KD, Cho EC, Fabrication and characterization of pseudo-ceramide-based liposomal membranes. *Colloids Surf B Biointerfaces.*, 2009; 73(2): 207-211.
76. Danaei M, Dehghankhold M, Ataei S, Hasanzadeh Davarani F, Javanmard R, Dokhani A, Khorasani S, Mozafari MR, Impact of Particle Size and Polydispersity Index on the Clinical Applications of Lipidic Nanocarrier Systems. *Pharmaceutics*, 2018; 10(2): 57.
77. Lúcio M, Giannino N, Barreira S, Catita J, Gonçalves H, Ribeiro A, Fernandes E, Carvalho I, Pinho H, Cerqueira F, Biondi M, Lopes CM, Nanostructured Lipid Carriers Enriched Hydrogels for Skin Topical Administration of Quercetin and Omega-3 Fatty Acid. *Pharmaceutics*, 2023; 15(8): 2078.
78. Kamel AE, Fadel M, Louis D, Curcumin-loaded nanostructured lipid carriers prepared using Peceol and olive oil in photodynamic therapy: development and application in breast cancer cell line. *Int J Nanomed.*, 2019; 14: 5073-5085.
79. Joshi A, Kaur J, Kulkarni R, Chaudhari R, *In-vitro* and *Ex-vivo* evaluation of active ingredient hydrochloride delivery using nano-transfersome based formulations.*J Drug Deliv Sci Techn.*, 2018; 45: 151-158.
80. Khan MI, Yaqoob S, Madni A, Akhtar MF, Sohail MF, Saleem A, Tahir N, Khan KU, Qureshi OS, Development and *In Vitro*/*Ex Vivo* Evaluation of Lecithin-Based Deformable Transfersomes and Transfersome-Based Gels for Combined Dermal Delivery of active ingredient and active ingredient. *Biomed Res Int.*, 2022; 2022: 8170318.
81. Mircioiu C, Voicu V, Anuta V, Tudose A, Celia C, Paolino D, Fresta M, Sandulovici R, Mircioiu I, Mathematical Modeling of Release Kinetics from Supramolecular Drug Delivery Systems. *Pharmaceutics*, 2019; 11(3): 140.
82. Trucillo P, Drug Carriers: A Review on the Most Used Mathematical Models for Drug Release. *Processes*, 2022; 10(6): 1094.
83. Bayer IS, Controlled Drug Release from Nanoengineered Polysaccharides. *Pharmaceutics*, 2023; 15(5): 1364.